Integration of Solar Power and Microwave WPT Exploiting Transparent Antennas

Published Version:
Gok, A.B., Masotti, D., Costanzo, A. (2023). Integration of Solar Power and Microwave WPT Exploiting Transparent Antennas. NEW YORK, USA : IEEE [10.1109/WPTCE56855.2023.10215619].

Availability:
This version is available at: https://hdl.handle.net/11585/943155 since: 2023-09-27

Published:
DOI: http://doi.org/10.1109/WPTCE56855.2023.10215619

A. B. Gok, D. Masotti and A. Costanzo

Integration of Solar Power and Microwave WPT Exploiting Transparent Antennas

In: 2023 IEEE Wireless Power Technology Conference and Expo (WPTCE), San Diego, CA, USA, 2023

The final published version is available online at:

https://doi.org/10.1109/WPTCE56855.2023.10215619

Integration of Solar Power and Microwave WPT Exploiting Transparent Antennas

A. Baris Gok
DEI "Guglielmo Marconi"
University of Bologna
Bologna, Italy
baris.gok@unibo.it

Diego Masotti
DEI "Guglielmo Marconi"
University of Bologna
Bologna, Italy
diego.masotti@unibo.it

Alessandra Costanzo
DEI "Guglielmo Marconi"
University of Bologna
Cesena, Italy
alessandra.costanzo@unibo.it

***Abstract*—This paper presents an integrated system for concurrent wireless power transfer and solar powering by means of a unique transparent antenna array which is obtained by an additive printing process on borosilicate glass. The optical transparency of the proposed 2-element microstrip patch antenna array, operating at 2.4 GHz, is achieved by the meshing technique. To ensure sufficient radiation property and optical transmittance, the design with 68.6% theoretical transparency and 6.9 dB simulated antenna gain is chosen. Moreover, the exploitation of the conductive layer as a ground plane of the antenna inside the solar cell has been validated by the measurements while resulting further compactness into the system. The subsequent solar power readings demonstrate that the printed meshed antenna arrays are suitable for integration with solar panels especially in energy cooperative in-space applications.**

***Index Terms*—additive printing, meshed antenna arrays, optically transparent antennas, wireless power transfer.**

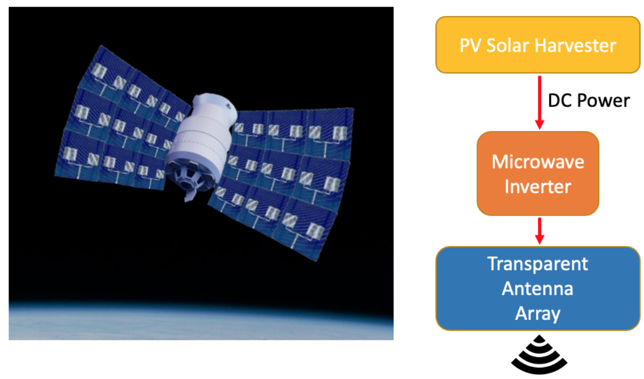

(a) (b)

Fig. 1. (a) Visual representation of a multi-layer satellite solar panel integrating microwave transparent antenna array. (b) Block representation of the solar panel-microwave power transmission system integration exploiting a transparent antenna array.

I. Introduction

Due to the rise of global warming and increasing energy consumption, the development of renewable energy harvesting systems is the greatest technological design challenge in recent years. Not only for sustainable future but also to eliminate the battery dependency and issues due to energy shortage, power harvesting mechanisms have been introduced and currently, solar power harvesting is the largest reported amount of energy per area in outdoor environments. However, solar power technology still has certain disadvantages, such as low energy efficiency, a heavy reliance on sunlight, and numerous other drawbacks. In this case, wireless power transfer (WPT) and solar power technologies can be integrated for more robust system.

The concept of transparent antennas first relates to an invention [1] for a window antenna that uses a transparent and conductive film to receive TV broadcast and FM signals. In the 21st century, transparent antennas have been continuously improved for integration with smart wearable devices [2], next generation communications [3] and satellite applications [4]. The two main types of optically transparent conductive techniques are transparent conducting films (TCFs) and conductive meshes [5]. TCFs are most frequently made of indium tin oxide (ITO) which has been studied intensively by industry and academia. Nevertheless, indium is extremely toxic when being manufactured, and inhaling it can be extremely dangerous. The latter, which concerns the fabricated design of this paper, is made up of a grid of transmissive conducting wires that was created by removing the conducting material from the structure's contour.

A promising future is ahead for transparent antennas in wireless communication systems but the integration with solar cells makes them applicable also for WPT systems. In some situations, solar power production might not function [6] or cannot be enough for high performance, energy-hungry applications. An effective integration of these two harvesting methods would increase the reliability of the total power production system and save valuable surface space for any type of battery dependent device. For the antennas to work correctly, the presence of solar cells must not considerably diminish the antennas' effectiveness and the solar cells must not be blocked by the antennas. Therefore, it is a key challenge to ensure compatibility of the transparent antennas and solar cells.

In this paper, a novel 2-element meshed transparent patch antenna array is proposed for WPT applications at 2.4 GHz. The meshed radiating elements and feeding network have been printed using Voltera V-One circuit printer on the surface of the high quality borosilicate glass Schott BOROFLOAT 33. The paper addresses the advantages of the antenna integrated

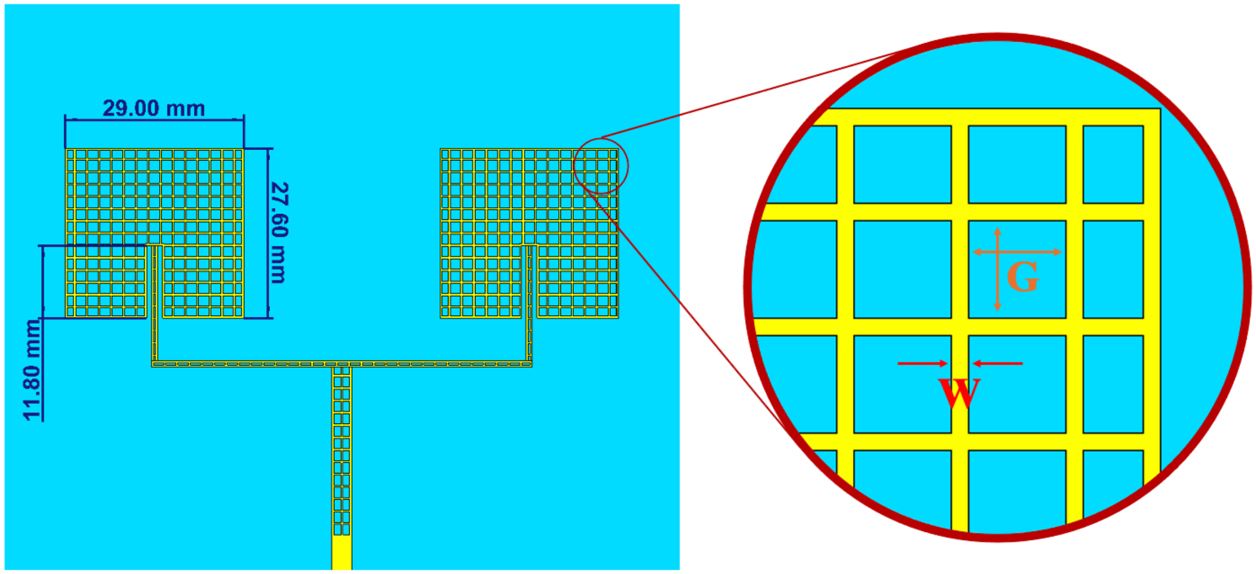

Fig. 2. The geometry of the designed antenna array and the description of the design variables.

solar cells with the unique usage of photovoltaic cell as a ground plane of the antenna. The optimization of the meshed transparent antennas and the validation of its performance with the measurements are the main objectives of this study. The eventual intention of this work, as depicted in Fig. 1, is to construct a large transparent rectenna which consists of high number of meshed antenna elements for integration of WPT with large solar panels especially for in-space satellite applications.

II. Meshed Antenna Design and Simulation

In order to increase the antenna gain, two element patches have been constructed onto the square BOROFLOAT33 substrate with the dimensions of 11 x 11 cm, which is the approximate upper limit by the printer capability. The BOROFLOAT33 glass has been chosen because of its high light transmission ($\approx$ 92%) in the visual wavelength range, optimal thermal resistance, and reliable mechanical strength [7]. For L and S band frequencies, the specified dielectric properties (ϵ_r = 4.6, tan(δ) = 0.007) of the substrate have been ensured via experiments with several 1-port and 2-port prototypes realized on samples 1.75 mm-thick.

The 2-element meshed transparent patch antenna array has been designed in a full-wave electromagnetic simulation program, CST Microwave Studio. Starting from a solid patch which served as the basis to obtain approximate dimension for the resonance frequency of interest, the meshing technique was utilized. Fig. 2 shows the geometry of the fabricated antenna with the patch dimensions where G and W are the gap width and the line width, respectively. As Fig. 2 indicates, the gap width is smaller near the edges of the patch in order to be fitted into the patch dimensions which is determined by the frequency of interest, 2.4 GHz. Meshed radiating elements and meshed feeding network, which includes two branches of 100 Ω from the antenna elements into the main 50 Ω line, have been included in the design. However, there is a section of solid transmission line to allow SMA connector to be soldered on. Subsequently, ground plane has not been printed since the conductive layer inside the solar panel, which will be placed on the back of the antenna, would act as a ground in the final setup.

The filling factor is an important parameter to optimize for the optical transparency of the antenna and defined as W/(W+G) [8]. Since the overall theoretical optical transparency T_{ant} of the antenna also depends on the substrate transmittance T_{sub}, it can be expressed as follows:

$$T_{ant} = T_{sub}(1 - \frac{W}{W+G})^2 \quad (1)$$

As it can be observed from the above equation, low filling

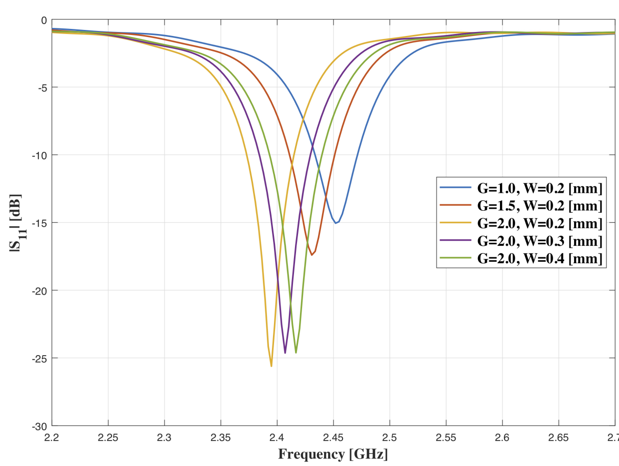

Fig. 3. Simulated reflection coefficients of the meshed antenna array with different gap width G and line width W.

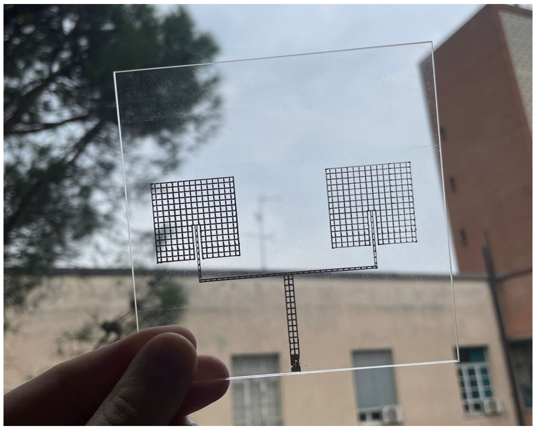

Fig. 4. The photo of the printed meshed antenna array.

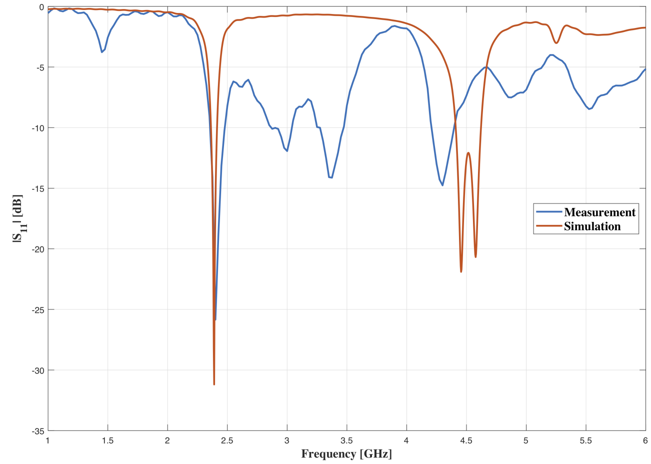

Fig. 6. The simulated and measured reflection coefficient plots.

factor is desirable for high optical transparency. It is important to point out that optical transparency concerns the transmission of optical wavelengths from the ultraviolet to infrared [5] and the line width W is limited by the resolution of the printer.

Several meshing structures are simulated where the width and length dimensions of the patches are kept constant but the line width and gap width were varied. Fig. 3 shows frequency shift on reflection coefficient as mesh variables are varied. The resonance frequency dropped as the gap width increases and the line width decreases. Further analysis of the antenna performance has been shown in Table I which indicates the simulated antenna gain, radiation efficiency at 2.4 GHz, and the calculated optical transparency with the above-mentioned meshing variables. The overall theoretical optical transparency T_{ant} is computed from (1), where the substrate transmittance T_{sub} is taken as 92% by the transparency of the BOROFLOAT33 glass. As the gap width increased, the transparency increased but antenna gain and radiation efficiency decreased. Subsequently, increasing the line width results on a decrease in transparency but an increase on antenna gain and radiation efficiency. This means that a trade-off between transparency and performance is needed: the selected array layout provides a 68.6% of optical transparency using G = 2.0 mm and W = 0.3 mm.

Table I
SUMMARY OF ANTENNA PERFORMANCE

Mesh Variables		**Performance Parameters**		
G [mm]	***W [mm]***	***Gain [dB]***	***Rad. Eff. [%]***	T_{ant} ***[%]***
1.0	0.2	7.4	74.8	63.9
1.5	0.2	7.1	71.6	71.6
2.0	0.2	6.6	68.0	76.0
2.0	0.3	6.9	70.5	68.6
2.0	0.4	7.1	71.9	61.6

III. ANTENNA FABRICATION AND MEASUREMENT

The proposed meshed microstrip antenna array is fabricated using Voltera V-One printer on a BOROFLOAT33 substrate with 1.75 mm thickness. The flexible conductive ink composed of tin, bismuth, and silver is directly printed on the glass for

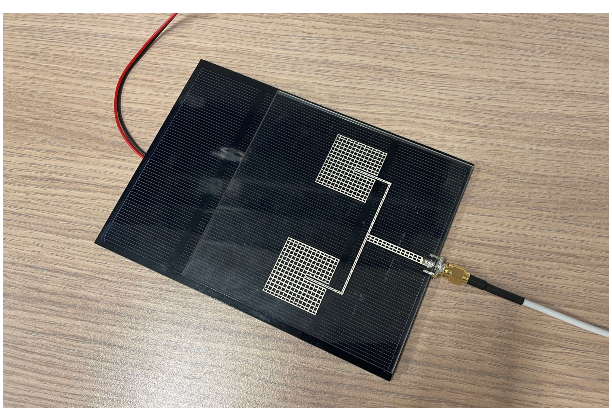

Fig. 5. The photo of the antenna measurement setup with the presence of solar cell.

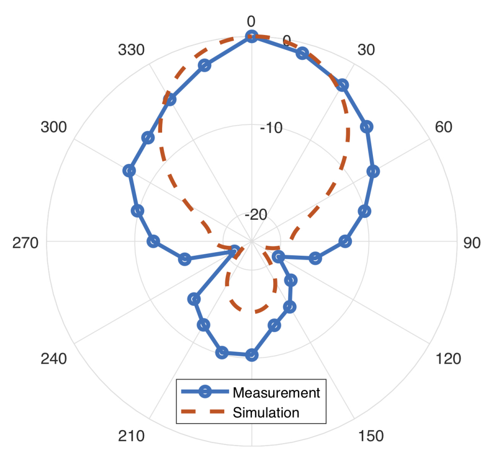

Fig. 7. The normalized radiation pattern of simulation and measurement in the H-plane.

10 minutes and cured at 160°C for 45 minutes. Fig. 4 shows the fabricated antenna which highlights its transparency.

A. Comparing Experimental and Simulated Results

As it is mentioned in the previous sections, the meshed antenna has been placed on top of the solar panel whose aluminium layer would act as a ground plane of the antenna. The setup of the antenna measurement is shown in Fig. 5 and the corresponding simulated and measured reflection coefficients S_{11} between 1-6 GHz are given in Fig. 6. One should pay attention to the fact that the layer representation of the panel has not been known exactly and the simulation has been done with the assumption of glass, silicon and aluminium materials. Therefore, the measurement result well agrees at the desired frequency but some discrepancies exist at certain regions because of the unknown solar cell stack-up. Furthermore, the normalized radiation pattern comparison is given in Fig. 7 where minor differences could be caused by the imperfect fabrication of the printer and model of solar panel in simulation.

B. Effect on Solar Cell Performance

In order to demonstrate the light transmission efficiency of the fabricated prototype and the power production change of a solar cell, measurements using 2.5 W solar panel made of single-crystal material with the dimensions of 160 x 116 x 2.5 mm are performed. It has a fine resin surface and solar energy transformation efficiency of 17%. The open-circuit voltage and short-circuit current readings of the solar panel, with and without the transparent antenna placed above, have been taken. Using the setup that is shown in Fig. 5 where the antenna is present, the measured short-circuit current and open-circuit voltage values of the panel have been recorded as 230 mA and 6.24 V. Table II shows also the cases where there is only glass substrate without the microstrip antenna and solar panel only. Comparing the DC performance of the solar panel only, generating a short-circuit current of 270 mA and an open-circuit voltage of 6.39 V, the use of the transparent meshed antenna array brings a decrease of 14.8% in the short-circuit current with a very minor drop of 2.3% in the measured open-circuit voltage. It should be noted that 11 x 11 cm antenna only covers approximately 70% of the solar surface. These preliminary results thus confirm the feasibility of the proposed combination of transparent antennas and solar panels.

Table II
SOLAR CELL MEASUREMENTS

	Open-circuited Voltage [V]	*Short-circuited Current [mA]*
Solar Panel Only	6.39	270
Solar Panel and Glass Only	6.32	250
Solar Panel and Transparent Antenna	6.24	230

IV. CONCLUSION AND FUTURE WORK

In this work, the possibility of implementing a multilayer structure capable of integrating solar cells with antennas systems, made with grating and printing techniques directly on the glass or on the superstrate of the solar cell has been presented and experimentally verified. Solar power and WPT integration is achieved by means of proposed meshed transparent antenna array.

This first proof-of-concept demonstrate that it is possible to create microwave antenna arrays by exploiting the same area of existing solar cells to realize the microwave energy harvester or re-transmission of the power accumulated by the cells, by including appropriate RF-to-DC converters between the two overlapping layers. The performance of the integrated system undergoes a limited degradation, if the metal pattern of the antennas is carefully optimized. The procedure adopted for the printed array has been validated by measurements and can be straightforwardly scaled for a large-element meshed antenna array. With the integration of a rectifier module into the large transparent antenna array, a complete WPT solar rectenna system is planned in the future. The system can be integrated on board nano or pico satellites for energy cooperative purposes.

REFERENCES

[1] H. Inaba, M. Shinnai, K. Nishikawa, T. Saitoh, and T. Tsukada, Vehicle window glass antenna using transparent conductive film, US Patent 4,849,766, 1989.

[2] C.-Y. Chiu, S. Shen, and R. D. Murch, “Transparent dual-band antenna for smart watch applications,” in *2017 IEEE International Symposium on Antennas and Propagation & USNC/URSI National Radio Science Meeting*, 2017, pp. 191–192.

[3] M. Stanley, Y. Huang, H. Wang, H. Zhou, A. Alieldin, and S. Joseph, “A Transparent Dual-Polarized Antenna Array for 5G Smartphone Applications,” in *2018 IEEE International Symposium on Antennas and Propagation & USNC/URSI National Radio Science Meeting*, 2018, pp. 635–636.

[4] C. Kocia and S. V. Hum, “Optically transparent reflectarray for satellite applications,” in *The 8th European Conference on Antennas and Propagation (EuCAP 2014)*, 2014, pp. 1607–1610.

[5] Z. J. Silva, C. R. Valenta, and G. D. Durgin, “Optically Transparent Antennas: A Survey of Transparent Microwave Conductor Performance and Applications,” *IEEE Antennas and Propagation Magazine*, vol. 63, no. 1, pp. 27–39, 2021.

[6] A. Costanzo, L. Roselli, A. Georgiadis, N. Carvalho, A. Takacs, P. Arpesi, and R. Martins, “Could the space probe philae© be energized remotely?” *Wireless Power Transfer*, vol. 6, pp. 1–7, 05 2019.

[7] ”BOROFLOAT Technical Details”, SCHOTT. [Online], Available: https://www.schott.com/en-au/products/borofloat-p1000314/technical-details. [Accessed: 15-Feb-2023].

[8] P.-C. Yu, C.-C. Hong, and T.-M. Liou, “Bendable transparent conductive meshes based on multi-layer inkjet-printed silver patterns,” *Journal of Micromechanics and Microengineering*, vol. 26, p. 035012, 03 2016.